Talanta Open 13 (2026) 100633

Contents lists available at ScienceDirect

Talanta Open

journal homepage: www.sciencedirect.com/journal/talanta-open

A sensitive and compact on-site and real time quantitative detection of foodborne and clinical pathogens by on-chip qPCR

Ana João Pereira [a,1], Steven Schoonderwoerd [a,1], Rodrigo Sergio Wiederkehr [b], Daniele Chieffi [c], Vincenzina Fusco [c], Gabriela Vollet Marson [a,*]

[a] IMEC the Netherlands, OnePlanet Research Center, Bronland 10A, 6708 WH Wageningen, the Netherlands
[b] IMEC, Kapeldref 75, 3001, Leuven, Belgium
[c] Institute of Sciences of Food Production, National Research Council of Italy (CNR-ISPA), 70126 Bari, Italy

ARTICLE INFO

Keywords:
DNA quantification
Silicon biochip
Molecular diagnostics
Food safety
Biosensor
Foodborne pathogens
Emerging pathogens

ABSTRACT

Herein we report the quantitative detection of pathogenic bacteria by an on-chip qPCR previously developed for COVID-19 detection, using *Staphylococcus aureus* as pilot microorganism. A conventional qPCR assay for the rapid and sensitive detection of *Staphylococcus aureus* harbouring the enterotoxin gene cluster (*egc*) was transferred to a microfluidic platform. Patterned silicon substrates were used as reaction vessels during on-chip qPCR. Reagent optimization was achieved through Design of Experiments (DoE), using multifactorial analysis with fractional factorial and central composite rotatable designs. On-chip thermal cycling and optical inspection were achieved using a compact reader providing real-time monitoring and accurate quantification. Experiments were performed to evaluate optimal assay efficiency, sensitivity, specificity, practicability, and robustness. The assay was tested for probe-based or intercalating dye-based amplification systems as those are fastest and most sensitive. Seven relevant components in the reaction mixture were screened through 16 amplification runs, where cost, speed and amplification quality were assessed. The screening identified the intercalating dye-based system as most promising, with polymerase and primer concentrations as the most influential factors. The following optimization design led to bacterial screening with template concentrations ranging from 4 to 40,000 copies in 1.8 μL of mixture per reaction under 19 minutes, compared to 10 μL of mixture per reaction under 40 minutes of run time using the conventional real time PCR platform. The workflow introduced here simplifies the transfer of qPCR recipes to microfluidic devices targeting faster results when compared with the current gold standard benchtop methods on pathogen detection in real time at on-site locations.

1. Introduction

In recent decades, there has been a growing trend in the development of sensitive, rapid and reliable methods to detect microorganisms and toxins in food, since large-scale production and distribution can threaten large populations when contamination occurs. Currently, the detection of pathogens in clinical and food systems is done through culture-based cultivation techniques, enzyme-linked immunosorbent assay (ELISA) and quantitative polymerase chain reaction (qPCR) [1–6]. Culture-based cultivation techniques remain the current standard for bacterial detection in a wide variety of foods due to their availability, low cost, and regulatory acceptance (e.g., WHO, FDA, FAO). Standard procedures for detecting Salmonella, *Escherichia coli*, and Listeria monocytogenes rely on selective enrichment and plating, followed by biochemical or serological confirmation. However, these methods typically require 18–48 hours or longer, are labour-intensive, and often delay critical interventions, complicating timely outbreak control across food sectors [7–11].

Molecular diagnostic tools such as qPCR have increased in popularity due to rapid, specific, and sensitive analysis of microbial DNA. These benefits make it attractive, especially when screening a larger number of samples. Among amplification systems for DNA quantification, there are probe-based and dye-based techniques. Intercalating dyes bind to newly formed double-stranded DNA and then undergo a conformational change that enhances their emitted fluorescence [12]. For the KAPA2G polymerase, EvaGreen is used as the dye. Although intercalating dyes

* Corresponding author.
E-mail address: gabriela.volletmarson@imec.nl (G.V. Marson).
[1] These authors have equally contributed to this work.

https://doi.org/10.1016/j.talo.2026.100633
Received 21 November 2025; Received in revised form 19 January 2026; Accepted 25 February 2026
Available online 26 February 2026
2666-8319/© 2026 The Authors. Published by Elsevier B.V. This is an open access article under the CC BY-NC-ND license (http://creativecommons.org/licenses/by-nc-nd/4.0/).

are usually more sensitive, they can also bind to double-stranded DNA fragments that are not relevant, such as primer-dimers. Therefore, a post-processing step using melting curve analysis is necessary to assess the origin of the measured fluorescence as signal from the desired amplified region of interest.

Alternatively, TaqMan is a probe-based amplification system, which uses single-stranded DNA or RNA molecules as probes that bind to the region of interest. These probes contain a reporter dye and a quencher of the signal. The probes attach to their complementary DNA sequence and subsequently get cleaved by the polymerase during the extension phase of amplification. Only after cleaving do the probes emit their fluorescence. By exclusively binding to the target sequence, probe-based assays enhance specificity and guarantee the fluorescence signal originates from the desired amplicon. In recent years, micro- and nano-fabrication technologies, originally developed for producing silicon-based chips for the microelectronics industry, have spread out in a variety of applications as chemical and biochemical tools, commonly referred to as Biomedical or Biological Micro-Electro-Mechanical Systems (Bio-MEMS). Obvious advantages of the miniaturized integrated detection technologies include higher sensitivity, as well as reduced reagent and sample volumes, reducing associated costs and time to result. Nevertheless, for lower reaction volumes, an assay optimization is needed to achieve similar amplification efficiency and reliability as observed in commercial benchtop tools. Moreover, the reagent concentrations adjustments and the addition of ingredients to minimize the increased impact of surface-to-volume ratio become prominent in smaller reaction qPCR screenings [13]. The optimization protocols paved the way for on-chip qPCR. Microfluidic chips have smaller thermal mass compared to the 96-well plates that are commonly used for qPCR benchtop tools, making the on-chip amplification routine suitable for faster thermal cycling [2]. Moreover, by utilizing chips made on substrates with good thermal conductivity, the total amplification time can be reduced to under 9 min or even 5 min, making this method suitable for ultra-fast diagnostics [14,15].

Microfluidic chip technology has progressed from simple fluid-handling devices to highly integrated platforms enabling rapid and sensitive pathogen detection. Recent developments include centrifugal microfluidic systems for recombinase polymerase amplification (RPA) and dual-mode nanozyme-based chips for colorimetric and bioluminescent detection of pathogens such as *Salmonella typhimurium*, achieving detection limits as low as 33 CFU/mL within 40 min [16,17]. Advances such as these leverage miniaturization, reduced reagent consumption, and portability, offering significant advantages over conventional methods like ELISA, lateral flow assays, and bulk PCR, which are often time-consuming, reagent-intensive, and less amenable to point-of-care use. Alternative microfluidic approaches, including isothermal amplification and CRISPR-based systems, provide speed and specificity but face limitations in quantitative accuracy, thermal uniformity, and multiplexing capability [18]. In contrast, microfluidic qPCR platforms overcome these challenges by integrating precise thermal cycling and real-time fluorescence detection within nanolitre-scale chambers, enabling accurate quantification, high specificity, and robust multiplexing. This combination of speed, sensitivity, and quantitative reliability positions microfluidic qPCR systems as superior solutions for pathogen detection in clinical and field settings.

Staphylococcus aureus is a ubiquitous bacterial pathogen known for its capacity to cause a wide range of human diseases, facilitated by its production of diverse virulence factors, notably staphylococcal enterotoxins (SEs). These toxins, alongside with other exotoxins like toxic shock syndrome toxin-1, contribute to serious foodborne intoxications, toxic shock syndrome, and staphylococcal scarlet fever, underscoring the significant public health burden associated with *S. aureus* infections [12–15]. While *S. aureus* is inactivated by cooking or pasteurization processing, its enterotoxins are heat-stable and remain active upon reaching the human gastrointestinal tract [19]. The enterotoxin production increases within an optimal temperature range of 20–37 °C and pH 4.0–7.4 with consequent release in foods [20]. A high number of SEs and staphylococcal enterotoxin-like toxins (SEls) have been discovered apart from the five classical SEs (SEA-SEE) [21]. *S. aureus* strains harbouring the so-called enterotoxin gene cluster (*egc*) operon have been found to cause staphylococcal food poisoning [22–25]. Moreover, these *egc*+ strains play a key role in clinical and subclinical mastitis as well as in other clinical diseases, thus prompting the need for a rapid and reliable method to detect *egc*+ *S. aureus* strains [26–28].

This paper proposes and evaluates a comprehensive validation framework for the qPCR detection and quantification of *egc*-positive *S. aureus* from food and clinical samples by using a custom microfluidic chip and instrument designed by a commercial partner (miDiagnostics, Leuven, Belgium). During validation, the applicability, specificity, sensitivity, and robustness were investigated for detection in complex matrices. By addressing challenges inherent to on-chip qPCR, we aim to provide a method that supports integration into clinical diagnostics and food safety monitoring, thereby enhancing our ability to detect and mitigate pathogens contamination in real-time scenarios. The successful validation of this technology offers transformative solutions for on-site rapid pathogen detection and contributes to improved public health and food safety strategies.

2. Materials and methods

2.1. Material

2.1.1. Bacterial strains and growth conditions

As proof of concept, DNA of 59 bacterial strains comprising foodborne and clinical *egc*+ (n = 25) and *egc*- (n = 13) S. *aureus* strains previously characterized by Fusco et al. [29] and Chieffi et al. [21], as well as strains belonging to other staphylococcal species (n = 12) and strains belonging to other genera (n = 9) were utilized in the present study (Supplementary Table A1). All bacterial strains were stored at the Institute of Sciences of Food Production National Research Council of Italy as pure glycerol (20 % v/v) stock cultures (−80 °C). Stock cultures were streaked on Baird Parker agar with egg yolk tellurite emulsion (Oxoid, Basingstoke, United Kingdom) incubated at 37 °C for 24–48 h (for staphylococcal species) or relevant (selective) agar media (for non-staphylococcal species). Working cultures were obtained inoculating single colonies in brain heart infusion broth (Oxoid, Basingstoke, United Kingdom) with 0.6 % yeast extract (Oxoid, Basing-stoke, United Kingdom). One mL aliquots were used for DNA extraction. DNA extraction was performed following the alcohol-based method described by Chieffi et al. [30], utilizing lysostaphin (Sigma-Aldrich, St. Louis, MO, USA) for staphylococcal species (8 μg/ml final concentration) and lysozyme (Sigma-Aldrich, St. Louis, MO, USA) for non-staphylococcal species (8 mg/ml final concentration).

2.1.2. Oligonucleotides and qPCR reagents

In this study, the primers and probe previously designed by Fusco et al. [29] were used. In particular, the set of primers *egcAUf/egcAUr* (Supplementary Table A2A) was synthesized by Sigma Aldrich (sigmaaldrich.com/oligos) and used for amplifying an 82 bp fragment of the *S. aureus egc* operon. The internal minor groove binder (MGB) Taq-Man probe (Supplementary Table A2B) was synthesized by Sigma Aldrich (sigmaal-drich.com/oligos). It contained the fluorescent reporter dye 6-carboxy-fluorescein (FAM) and an MGB group at the 3′ end. The MGB is added to the probe to increase stability and specificity of probe hybridization and enhance fluorescent performance.

The TaqMan system utilized AmpliTaq Gold DNA polymerase (Fisher Scientific, Hampton, USA), while the intercalating dye system employed KAPA2G Fast HotStart polymerase (Roche, Basel, Switzerland) with fluorescent detection facilitated by EvaGreen dye 20X (25 μM; VWR, West Chester, USA), whereas TaqMan relied on specific probes for signal generation (Supplementary Table A2B). Magnesium chloride ($MgCl_2$), deoxynucleotide triphosphates (dNTPs) and PCR-grade water were

provided by Sigma-Aldrich (St. Louis, USA), and bovine serum albumin (BSA) was procured in Roche (Basel, Switzerland).

2.1.3. On-chip qPCR system

2.1.3.1. Microfluidic chip. The chips used in this study were supplied by MiDiagnostics (Leuven, Belgium). The design of the chip consists of a meandered channel (200 μm width, 3000 μm length and 200 μm depth, 1.8 μL as total volume) used as reaction chamber with an inlet hole (0.5 mm diameter) at each end. The channels were fabricated on a 10 × 5 mm silicon substrate by combining conventional photolithography with dry etching techniques sealed by an anodic bonded cover glass. After fabrication, the chip was attached to a frame (20 × 70 mm in size) for easier manipulation and connected to a plastic foil of 33 × 20 mm containing an embedded channel of 2 mm by 120 mm of length (with a total volume of 4.8 μL) which was aligned to one of the chip inlets in use to facilitate injection of reagents. As a final step, the assembled chip went under an oxygen plasma furnace for 30 min at 80 W power (Mini-Flecto, Plasma Technology, Herrenberg-Gültstein, Germany) to remove any possible organic residues acquired from the storage period prior to usage. Fig. 1 shows the front and back of the chip after assembly, highlighting the location of the different elements.

2.1.3.2. Instrument for the on-chip quantification of S. aureus. On-chip qPCR was performed using a compact and portable instrument (16 cm length x 18 cm height x 16 cm width, weight: 5.35 kg, Fig. 2) acquired from MiDiagnostics (Leuven, Belgium), equipped with heating and optical modules for temperature control and fluorescence detection. The filters installed on the tool are compatible with green fluorescent protein/fluorescein amidite (GFP/FAM) fluorophores bands with excitation at the range of 480–500 nm and emission at 520–540 nm. The chips were inserted into the equipment by a slit located at the front panel. After loading the sample, the inlet ports are sealed and the chip inserted into an instrument that performs temperature cycling while acquiring fluorescence images. All the parameters related to the amplification step (temperature cycling, fluorescence images, and data acquisition) were controlled using a custom-made software installed on a peripheral computer.

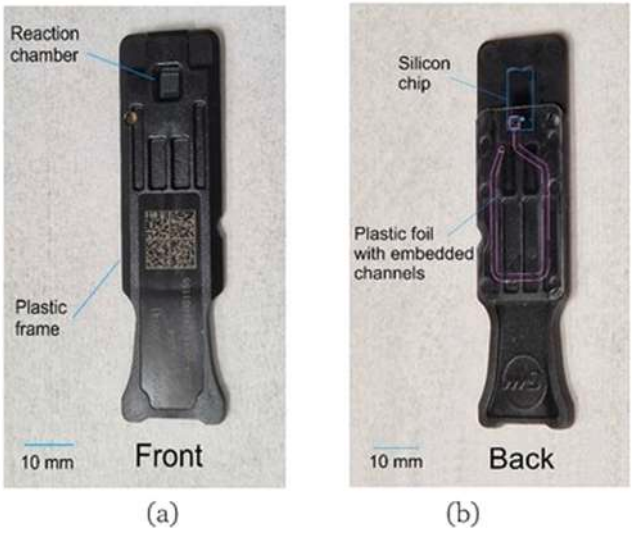

Fig. 1. (a) Front and (b) back side views of the chip after assembly. The plastic frame has an opening allowing the visualization of the reaction chamber during the temperature cycling.

Fig. 2. Instrument in use for on chip qPCR amplification step. The dimensions are 16 × 18 × 16 cm (length x height x width).

2.2. Methods

2.2.1. Benchtop qPCR for referencing

The same master mixes were tested on benchtop qPCR using the Bio-Rad CFX Opus 96 Touch Real-Time PCR System (Bio-Rad, Hercules, California, U.S.A) to validate results from the microfluidic chip. Three replicates of positive control (strain '367P', Supplementary Table A1) were tested for each recipe, along with two no template control (NTC) samples. Both benchtop and on-chip qPCR tools use the same thermal cycling program of dwell times (see Sections 2.2.2.3 and 2.2.2.4), but overall time on the benchtop tool is longer than on-chip due to longer ramp times between temperatures. Also, the volume on the benchtop is 10 μL, whereas the volume on-chip is 1.8 μL. Following benchtop amplification, melting curve analysis from 65 °C to 95 °C was performed to estimate PCR product size and presence of primer-dimers.

2.2.2. On-chip qPCR

2.2.2.1. Loading procedure. The reagents were inserted in the microfluidic chip (Supplementary Fig. A7a) by dispensing a 6 μL drop of the premixed reagents onto the plastic foil inlet. Then, the fluid was guided by capillary flow towards the reaction chamber (1.8 μL) through the fluidic channels present on the plastic interposer (Supplementary Fig. A7b). The filling procedure was completed in approximately 20 s. When the loading was successfully completed, an adhesive foil (polyimide film tape, catalogue code: 7000,144,792, 3M) was placed directly at the chip inlet- and outlet ports, sealing the microfluidics circuit during the qPCR temperature cycling (Supplementary Fig. A7c and d). Bovine serum albumin (BSA) is added to PCR solutions to stabilize polymerase enzymes and prevent adsorption of reaction components to chamber surfaces by competitively blocking polymerase binding [31,32].

2.2.2.2. Amplification curves data acquisition and validation. The fluorescence curves were generated by plotting reaction chamber's mean fluorescence intensity (relative fluorescence units, RFU) per temperature cycle. The data was compared with the benchtop tool results (acquired under similar temperature cycling dwell times) for performance validation.

2.2.2.3. On-chip qPCR reaction design (screening). A Fractional Factorial Design (FFD) is a solving method based on testing a subset of all possible combinations and levels of factors, rather than a full factorial design. By assuming that high-order interactions can be neglected, FFD helps

identify the most important factors for assay optimization with fewer runs. Thus, the optimization process started by determining the most influential ones on the following amplification systems: probe-based TaqMan, and intercalating dye EvaGreen with KAPA2G polymerase. For this purpose, two separate FFDs of seven factors (2^{7-3}, resolution IV) were employed, resulting in 16 runs each for each amplification system. During screening, the thermal cycling program consisted of initial denaturation for 3 min at 95 °C, followed by 40 cycles of denaturation for 10 s at 95 °C and elongation for 30 s at 60 °C. With ramp speeds of 7 °C/s, resulting in a total run time of approximately 37 min.

The choice of the seven factors was based on previous results and suppliers' information. The factors included in the design had two levels, lower (−1) and upper (+1) limits. These were usually set to 0.5 or 3 times the recommended concentration, respectively (see Table 1).

Outcome responses of the design were defined as: (1) the threshold cycle (Ct), and (2) a categorical grade of the curve fit over the data points. A full summary of the design with the uncoded levels for each run can be found in Supplementary Tables A3 and A4, for the TaqMan and KAPA2G amplification systems, respectively. All runs were performed in a randomized order.

2.2.2.4. On-chip qPCR reaction design (optimization). Following the reagents screening, an optimization design was employed to determine optimal concentrations when using KAPA2G as polymerase on the amplification reaction. Only the most influential factors on outcome measures were chosen. In the end, from the seven factors present on the screening experiment, only primer and polymerase concentrations were kept in the optimization. For this optimization, a central composite rotatable design (CCRD) was used. This is a response surface plot used in experimental design that is particularly useful for building models of second-order response surfaces and is known for its ability to provide uniform prediction errors across the design space. In this study, CCRD was used following response surface analysis methodology [33]. The design contained four factorial points, four axial points, and a centre point that was repeated five times, totalling 13 runs (see Supplementary Fig. A8). Remaining reaction components were added in the following concentrations: dNTPs (200 μM), BSA (3 mg/mL), $MgCl_2$ (6 mM), EvaGreen (3X) and KAPA2G buffer (1X) and microbial DNA-free water to an end volume of 1.8 μL per chip. Table 2 summarizes the tested recipes.

The kinetics experiments performed prior to the optimization (data not shown) demonstrated the functionality of a shortened thermal cycling program, reinforced by prior research reported by Cai et al. [15]. During optimization, the thermal cycling program consisted of initial denaturation for 1 min at 95 °C, followed by 40 cycles of denaturation for 1 s at 95 °C and elongation for 15 s at 60 °C. With ramp speeds of 7 °C/s, total run time resulted in approximately 19 min.

In the optimization design, the outcome measures of the tested recipes were the Ct value and PCR efficiency. To assess PCR efficiency and sensitivity, a dilution series of DNA template (strain 'NCTC 9393') was created to establish a standard curve of five points. The DNA dilutions were distributed around the predicted limit of detection, based on earlier experiments (data not shown). Around this limit, it was deemed most probable to determine differences in the limit of detection for the different recipes. Considering that one *S. aureus* genome equivalent equals to 3.03 fg [29], DNA concentrations started at 100 genome equivalents (303 fg) per reaction (GE/reaction), based on a reaction volume on-chip of 1.8 μL. Subsequent dilution points were 50, 10, 5 and 2.5 GE/reaction.

Table 1
Selected factors and their final concentrations at manufacturer's recommendation levels, lower and upper limits chosen for the screening experiment of TaqMan and KAPA2G amplification systems.

Factor (unit)	Recommended	Lower limit	Upper limit
$MgCl_2$ (mM)	2	1	6
dNTPs* (μM)	200	100	600
BSA* (mg/mL)	1	0	3
AmpliTaq polymerase (U/μL)[1]	0.2	0.1	1
KAPA2G polymerase (U/μL)[2]	0.02	0.01	0.1
Forward primer (nM)	500	250	1000
Reverse primer (nM)	500	250	1000
Probes (nM)[1]	250	100	750
EvaGreen (X)[2]	1	0.5	3

* dNTPs: deoxynucleotide triphosphates; BSA: bovine serum albumin.
[1] Reagents in use for TaqMan system only.
[2] Reagents in use for KAPA2G only.

Table 2
Coded and uncoded optimization design. The centre point was repeated five times, hence recipes 9–13 are identical.

	Recipe	X1, Polymerase	X2, Primers	Polymerase (U/μL)	Primers (nM)
Factorial points	1	−1	−1	0.035	300
	2	1	−1	0.17	300
	3	−1	1	0.035	1300
	4	1	1	0.17	1300
Axial points	5	-α	0	0.005	800
	6	α	0	0.2	800
	7	0	-α	0.1	100
	8	0	α	0.1	1500
Centre point	9–13	0	0	0.1	800

2.2.2.5. On-chip qPCR reaction design (model validation). From the optimization data, DoE results were generated to correlate the polymerase and primer concentrations to the outcome measures. From these DoE results, three recipes were chosen to validate the model (Table 3). One recipe was chosen with expected bad outcome measures ("unreliable"). Two expected good recipes were chosen, one with a higher polymerase concentration (labelled as "high-cost") and the other with lower polymerase concentration (labelled as "low-cost"). These recipes were tested for the same DNA concentrations as the dilution series in the optimization experiment, ranging from 2.5 to 100 genome equivalents per reaction. Each dilution was tested in two replicates and one NTC as negative control. The average Ct values were determined, and PCR efficiency was calculated. From all three recipes the benchtop samples were stored post-amplification for primer-dimer analysis using gel electrophoresis. To assess the cost per recipe, the volume of each component required was multiplied by its price per microliter, based on bulk reagent pricing. This included polymerase, primers, BSA, dNTPs, and $MgCl_2$. Total cost per reaction was calculated separately for chip-based and benchtop formats, considering the lower reaction volumes on-chip, which notably reduce costs per test, especially for expensive reagents like polymerase. The detailed cost breakdown and calculations (€) can be found in the supplementary material (Supplementary Table A5).

2.2.2.6. Reproducibility and sensitivity. Following the validation of the model, the recipe chosen was the one whose variance was best explained by the model. In this case, the low-cost model was chosen to proceed to further analysis. During sensitivity, this condition was tested for 20 times at a DNA dilution suspected to be the Limit of Quantification (LoQ). Following quantification at 95 % certainty, a standard curve of 10-fold increases was generated, ranging from 4 to 4×10^5 genome equivalents per reaction.

2.2.2.7. Specificity. The approach described by Broeders et al. and the Codex Alimentarius [34,35] was followed to evaluate the specificity of on-chip qPCR assays. A panel of 20 known target and 20 non-target DNAs, highlighted in Supplementary Table A1, were tested. Target samples were run at 100 GE per reaction, while non-targets were tested at 1000 GE per reaction to help reveal any potential cross reactivity. All

Table 3
Overview of the validation recipes with coded (X1, X2) and uncoded (polymerase, primers) concentrations.

Recipe	X1, Polymerase	X2, Primers	Polymerase (U/μL)	Primers (nM)	Price per reaction on chip (€)	Price per reaction on benchtop (€)
High-cost	0.5	−0.75	0.135	430	0.902	1.504
Low-cost	−0.3	−1.25	0.08	180	0.645	1.076
Unreliable	−1.25	1.25	0.016	1400	0.367	0.612

samples were tested in duplicate. The results were expressed as a percentage of false positives or negatives using Eqs. (1) and 2.

$$False\ Negatives\ (\%) = \frac{100 \times Number\ of misclassified\ known\ positive\ samples}{Total\ number\ of\ known\ positive\ samples} \quad (1)$$

$$False\ Positives\ (\%) = \frac{100 \times Number\ of misclassified\ known\ negative\ samples}{Total\ number\ of\ known\ negative\ samples} \quad (2)$$

2.2.3. Electrophoresis

During validation, gel electrophoresis was performed in addition to melting curves to separate amplification products based on size. Benchtop qPCR post-amplification samples were run on a 2 % SeaKem® LE Agarose gel (Lonza, Walkersville, MD, USA), mixed with 1x TAE buffer (Tris, Acetic acid and EDTA) (Bio-Rad, Hercules, CA, USA). For size estimation, a GeneRuler™ Low Range DNA Ladder (ThermoFisher, Waltham, MA, USA) was added, since expected amplicon size was 82 base pairs.

2.2.4. Data analysis and statistics

2.2.4.1. Data acquisition. When performing on-chip qPCR, a routine was needed to retrieve the fluorescence curves. First, we imported the images from the thermal cycling program in ImageJ analysis program and selected the area of the images containing the meandering channels of the chip. Next, in ImageJ mean fluorescence intensity per pixel (RFU) was plotted by using the 'plot Z-axis' functionality. The raw data from these graphs was extracted using ImageJ and imported into Microsoft Excel, where it was first zero-normalized and then scaled to relative values ranging from 0 to 100. Data from benchtop qPCR was merely used as a rough estimate of Ct value and to check for amplification and primer-dimer presence. For this reason, the benchtop data was not normalized or used for further quantification, analysis, or comparison to on-chip qPCR results.

2.2.4.2. Data statistics. DoE were designed and processed using an R script developed in-house by our team (RStudio, version 4.4.1, R Core Team, 2024).

3. Results

3.1. On-chip qPCR reaction design (screening)

The TaqMan probe-based assay showed a large variance in results of different outcome measures as can be seen for both benchtop and on-chip qPCR results (see supplementary Table A6). In certain recipes – such as 3, 4, and 13 – substantial increases in fluorescence intensity were observed, with mean pixel intensity values rising by several thousand as measured by ImageJ. These recipes also exhibit low curve residual values on-chip and good categorical curve goodness of fit on benchtop. These qualities combined highlight their well performance.

In contrast, recipes 5, 10 and 14 exhibit negligible or poor amplification, as seen by their low fluorescence increases. Consequently, their Ct values could not be determined and have been manually entered as 45 to highlight poor performance of amplification. These recipes' poor performance is further highlighted by their poor categorical good of fit on both benchtop and on-chip qPCR results.

In Table 4, the results of the multifactorial analysis on the data from the TaqMan screening experiments can be observed. Polymerase showed significant impact on all outcome measures, except for curve residuals on-chip and the categorical goodness-of-fit of curves on benchtop data. The impact of polymerase was positive on all outcome measures, except for fluorescence increase on-chip. The concentration of both forward and reverse primers showed predominantly positive impact on most outcome measures. Notably, the impact of BSA was positive for outcome measures on-chip, such as fluorescence increase and the categorical goodness-of-fit of the curves. Wherever significant, the impact of $MgCl_2$ was always strongly positive. Contrarily, the influence of increased dNTPs concentration was strongly negative for the outcome measures where its impact was significant.

The screening experiment of the KAPA2G amplification system using EvaGreen as intercalating dye screened several recipes (see Supplementary Fig. A8). Recipes 5, 10, and 14 – exhibited extremely low fluorescence increases on chip, some even decreased relative to the starting pixel intensity values measured in ImageJ. Recipes exhibiting such low fluorescence values accordingly showed poor categorical goodness of fit on-chip, high curve residuals on-chip and received a manually entered Ct value of 45 to showcase poor amplification. Other trials - such as 3, 4, 7, 8, 11, 12 13 and 16 - showcased very high fluorescence increase. In turn, the overall results for these recipes were good categorical curve goodness of fit, low curve residuals on-chip and good performance on benchtop with Ct and categorical fit.

In Table 5, the results of the multifactorial analysis on the data from the KAPA2G screening experiments can be observed. The factor polymerase showed highly significant impact on all outcome measures, except for categorical fit of curves on benchtop data. Primers - both forward and reverse - showed little significant impact on any of the outcome, except for categorical fit of curves on benchtop for reverse primers and categorical fit of curves on-chip for forward primers. The intercalating dye, EvaGreen, only showed strongly positive impact on the increase in fluorescence on chip ($p < 0.1$). Bovine serum albumin showed strong positive impact on-chip for Ct ($p < 0.001$), fluorescence increase ($p < 0.05$) and categorical fit ($p < 0.01$). $MgCl_2$ showed strong positive impact for Ct on-chip ($p < 0.001$), Ct on benchtop ($p < 0.001$) and categorical curve fitting on-chip ($p < 0.01$). Influences from dNTPs were mostly non-significant, except for strong negative influences on Ct on-chip and on benchtop ($p < 0.001$).

After the screening, $MgCl_2$ and bovine serum album (BSA) were removed as factors because $MgCl_2$ is an essential co-factor to DNA polymerase and factors should be independent from each other. Additionally, BSA was no longer analysed as a factor, because it was deemed essential to the on-chip qPCR amplification. The surface chemistry of silicon can bind reaction chemicals and inhibit amplification, which was also suggested by the screening design analysis.

3.2. On-chip qPCR reaction design (optimization)

On-chip qPCR yielded no false positive amplification in any recipe. Benchtop qPCR showed false positive amplification for one NTC sample in recipes 3 and 1, and for both NTC samples in recipes 12 and 8. The positive controls in triplicate on benchtop qPCR showed consistent, qualitative amplification across repetitions for all recipes except one. For this recipe 5, the amplification displayed low fluorescence intensity, and no plateau was reached.

Table 4
Results of multifactorial analysis for the TaqMan probe-based amplification system. Displayed are the influence that each factor exerted on the mentioned outcome measure.

Factor	Ct On-chip	ΔFluorescence On-chip	Ct on Benchtop	Curve residuals on-chip	Categorical fit of curves benchtop	Categorical fit of curves on-chip
Polymerase	~	**	~	*n.s.*	*n.s.*	*
Primer (forward)	**	*	~	*n.s.*	**	*n.s.*
Primer (reverse)	~	**	*n.s.*	*n.s.*	*n.s.*	*
Dye (EvaGreen)	*n.s.*	*n.s.*	*n.s.*	*n.s.*	*n.s.*	*n.s.*
BSA	*n.s.*	**	*n.s.*	*n.s.*	*n.s.*	*
$MgCl_2$	***	**	*n.s.*	*n.s.*	*n.s.*	***
dNTPs	**	**	*n.s.*	*n.s.*	*	**

$p < 0.1$; * $p < 0.05$; ** $p < 0.01$; *** $p < 0.001$; *n.s.* non-significant.

Table 5
Results of multifactorial analysis for the KAPA2G system. Displayed are the influence that each factor exerted on the mentioned outcome measure.

Factor	Ct On-chip	ΔFluorescence On-chip	Ct on Benchtop	Curve residuals on-chip	Categorical fit of curves benchtop	Categorical fit of curves on-chip
Polymerase	**	*	***	**	*n.s.*	**
Primer (forward)	*n.s.*	*n.s.*	*n.s.*	*n.s.*	*n.s.*	**
Primer (reverse)	*n.s.*	*n.s.*	*n.s.*	*n.s.*	**	*n.s.*
Dye (EvaGreen)	*n.s.*	~	n.s.	*n.s.*	*n.s.*	*n.s.*
BSA	***	*	***	*n.s.*	**	**
MgCl2	***	*n.s.*	***	*n.s.*	*n.s.*	**
dNTPs	***	*n.s.*	***	*n.s.*	*n.s.*	*n.s.*

$p < 0.1$; * $p < 0.05$; ** $p < 0.01$; *** $p < 0.001$; *n.s.* non-significant.

During optimization, the on-chip qPCR amplification using KAPA2G polymerase with EvaGreen Dye was tested in nine recipes for sensitivity and PCR reproducibility. Benchtop qPCR has a positive control in triplicate and a non-template control (NTC) in duplicate. The nine recipes corresponded to the four factorial points and four axial points, along with the centre point recipe that was repeated five times.

For on-chip qPCR, all recipes exhibited varying ranges of amplification throughout the different dilutions of starting DNA concentrations. Notably, the centre point recipes were repeated five times to test reproducibility and consistency but displayed differences in sensitivity and PCR efficiency (Table 6). To support the interpretation of the CCRD results, the full set of standard curves and efficiency calculations for all 13 recipes (summarized in Table 6) has been added to the Supplementary Materials (Supplementary Figs. A9 and A10). These figures show the effect of varying polymerase and primer concentrations on Ct values, PCR efficiency, and the overall response surface of the optimization.

Following false positive amplification on benchtop in NTC samples, melting curve analysis was added to the benchtop protocol. However, this analysis could not sufficiently rule out the cause of the signal. Therefore, agarose gel electrophoresis was performed to assess the size and possible origin of the amplicons.

A response surface model based on the C_t values and efficiency data from the CCRD matrix was built to guide further optimization. The model showed a clear trend: predicted PCR efficiency increased with higher primer concentrations and lower polymerase levels. This trend was visualized in a two-dimensional contour plot (Fig. 3A) and a three-dimensional surface plot (Fig. 3B). These visualizations were then used to select three representative recipes for follow-up: a high reagent "high-cost" condition predicted to yield robust amplification; a more economical "low-cost" condition; and a third recipe ("unreliable") that, while showing strong predicted efficiency, involved an extreme reagent combination that raised concerns about specificity.

During validation, two recipes ("high-cost" and "low-cost") displayed consistent and comparable C_t values over the dilutions (Table 7). Notably, the "unreliable" recipe that contained low polymerase and high primer concentrations showed earlier amplification than the former recipes. Additionally, the PCR efficiency of the "unreliable" recipe was closer to 100 %, which indicates this recipe might have the best outcome. However, benchtop qPCR and later on-chip qPCR results showed false positive amplification of the negative control (NTC) samples. Subsequent gel electrophoresis of benchtop qPCR samples post-amplification showed that the product size of false positive amplification differed slightly from the predicted amplicon of 82 bp (data not shown).

Table 6
Optimization results from on-chip qPCR experiments. C_t1 - C_t5 are the on-chip C_t values for the previously reported DNA dilutions ranging from 100 to 2.5 genome equivalents per reaction, respectively.

Recipe	Polymerase (U/μL)	Primers (nM)	C_t1	C_t2	C_t3	C_t4	C_t5	Efficiency	C_t Range[1]
1	0.035	300	31.2	32.0	32.5	34.6	–[2]	185.8	1–4
2	0.17	300	31.3	32.6	33.8	34.4	–[2]	186.9	1–4
3	0.035	1300	32.2	34.5	34.5	34.1	–[2]	687.1	1–4
4	0.17	1300	31.1	31.4	34.1	35.4	–[2]	96.5	1–4
5	0.005	800	33.6	33.9	–[2]	–[2]	–[2]	992.5	1–2
6	0.2	800	33.8	32.5	33.6	36.5	–[2]	222	1–4
7	0.1	100	35.3	36.2	–[2]	–[2]	–[2]	109	1–2
8	0.1	1500	31.3	32.4	34.0	35.9	-	104.6	1–4
9	0.1	800	32.2	33.4	36.1	34.3	40.0	83	1–5
10	0.1	800	32.1	33.1	35.6	36.7	37.4	97.2	1–5
11	0.1	800	33.1	33.9	34.4	35.7	–[2]	293.8	1–4
12	0.1	800	31.6	32.4	33.9	34.3	–[2]	193	1–4
13	0.1	800	34.2	35.1	37.1	–[2]	–[2]	122.1	1–3

[1] C_t range indicates which C_t values were used to calculate the PCR efficiency of the respective recipe.
[2] Lack of amplification or unreliable and were excluded from PCR efficiency calculations.

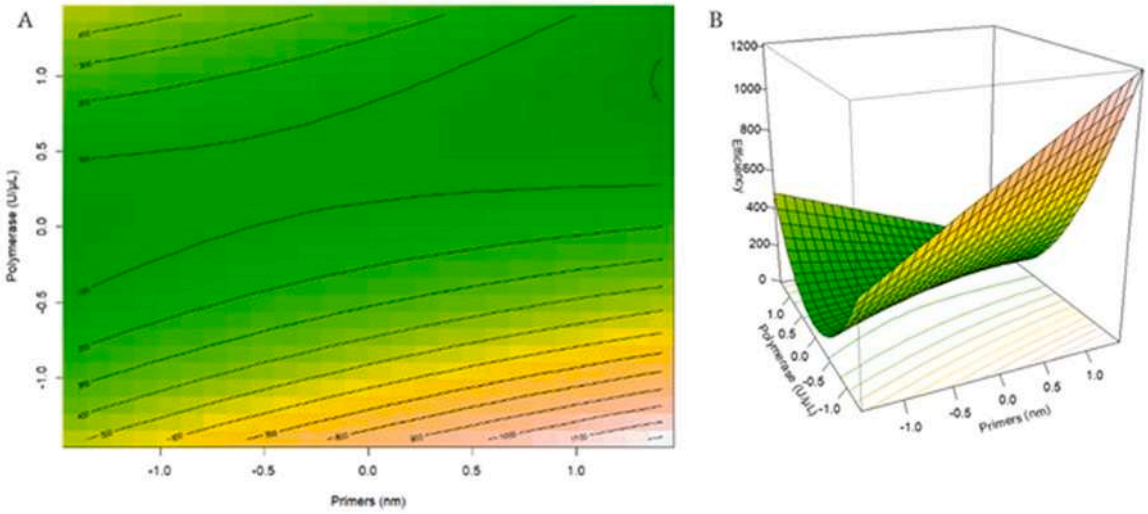

Fig. 3. Response surface plots from CCRD optimization showing predicted PCR efficiency as a function of primer and polymerase concentrations. A: Contour plot. B: 3D surface plot. The model was used to guide recipe selection for the validation experiments.

Table 7
Overview of the validation results.

Recipe	Run order	X1	X2	Polymerase	Primers	C_tS1	C_tS2	C_tS3	C_tS4	C_tS5	Eff1_5	Eff1_4	Eff1_3
High-cost	4	0.5	−0.75	0.135	430	31.46	32.55	33.63	34.97	34.04	250.0	157	206.6
Low-cost	2	−0.3	−1.25	0.08	180	31.6	32.78	34.13	35	33.44	326.6	138.1	158.5
Unreliable	3	−1.25	1.25	0.016	1400	28.77	30.40	32.26	34.85	33.535	98.4	72.5	99.1

The recipes are shown with corresponded coded (X1, X2) and uncoded (polymerase, primers) concentrations. C_t values are shown for the average of the repetitions at the dilution concentrations of 100 to 2.5 genome equivalents per reaction in C_tS1 to C_tS5, respectively. PCR efficiencies are calculated based on the dilutions 1–5, dilutions 1–4 and 1–3 for the Eff1_5, Eff1_4 and Eff1_3, respectively.

3.3. Efficiency and sensitivity

Following a short preliminary experiment, the suspected LOQ of our assay with KAPA2G polymerase and EvaGreen dye was four genome equivalents per reaction (1.8 µL). Out of 20 successful repetitions at this concentration, 19 produced a quantifiable signal that yielded a Ct value,

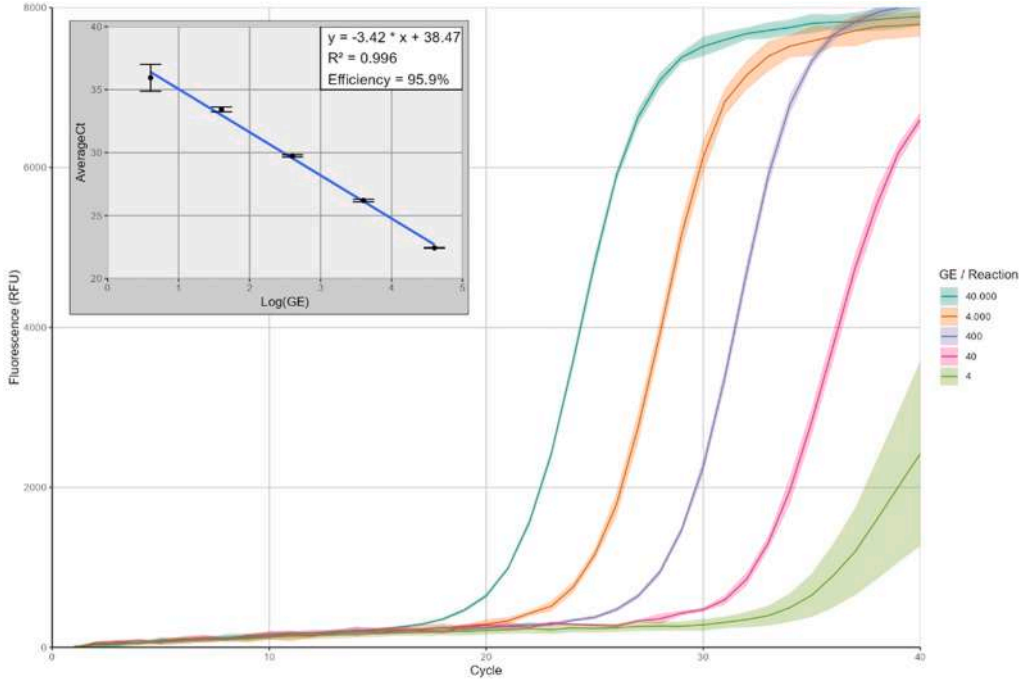

Fig. 4. Amplification curves following sensitivity experiments and dilution series performed on-chip. Lines represent the mean of all repetitions at that DNA concentration, with a surrounding band representing the standard deviation. The inset graph represents the average Ct value generated from the amplification curves, along with standard deviation. The resulting on PCR efficiency reached 95.9 %.

corresponding to a 95 % detection rate and establishing four genome equivalents per reaction as the LOQ95. To document assay behaviour across the lower concentration range, these 20 replicates were included in the sensitivity assessment. In addition, the standard curve was generated from 10-fold increases in starting DNA concentrations and tested in triplicate for each point. The corresponding plot includes error bars to illustrate replicate variability across the full dynamic range. This dilution series resulted in an on-chip PCR efficiency of 95.9 % (Fig. 4).

3.4. Specificity

This specificity assay evaluated the ability of the test to correctly identify target versus non-target sequences. The assay successfully detected 19 out of 20 targets, corresponding to a false negative rate of 5 % (strain '363P'), indicating high sensitivity. Among the 20 non-targets tested, 3 were detected ('372P', '373P' and 'CR1'), yielding a false positive rate of 15 %. While the assay demonstrates high specificity, the observed false positive rate suggests potential cross-reactivity with some non-targets, highlighting an area for further optimization to improve specificity.

4. Discussion

Quantitative polymerase chain reaction (qPCR) is an invaluable tool in microbiology and is also applied in food technology to detect food pathogens and increase food safety [3,29,36]. The interest of detecting foodborne pathogens is growing due to the increased incidence of foodborne illnesses in recent years [37]. Currently, different research groups are working to optimize sensitivity [5,38], specificity [39,40] and multiplexing [41,42] of conventional benchtop qPCR assays for bacteria detection. However, benchtop qPCR systems have a longer protocol, whereas new technologies facilitate rapid detection using on-chip technology [15]. Hence, there is interest in miniaturized instruments [43,44], making assay optimization on a microfluidic chip an important asset to investigate [45]. Here, we show the potential of silicon chips with a meandering channel as reaction chamber to perform on-chip qPCR for rapid detection of the bacterial pathogen *S. aureus* harbouring the enterotoxin gene cluster (*egc*). More specifically, multifactorial analysis and Design of Experiments (DoE) were applied to select an amplification system and optimize its reaction conditions for on-chip qPCR.

Several studies report reliable detection of *S. aureus* and other foodborne bacteria in milk, meat, poultry, and ready-to-eat products using standard qPCR chemistries [6,46–49]. These studies show that qPCR remains sensitive and specific even in the presence of typical food-matrix inhibitors, supporting the feasibility of applying our optimized on-chip assay once the consortium-generated isolates become available. Moreover, it is important to note that the primers and probe used for the on-chip qPCR proposed in the paper have been already successfully tested in a conventional real time PCR on spiked milk samples and have been validated on real raw milk samples by comparison with plating combined with conventional PCR [29].

Two widely used systems were compared: AmpliTaq with TaqMan probes, and KAPA2G with the intercalating dye EvaGreen. The AmpliTaq system is highly specific, because probe-based fluorescence only occurs when bound to the exact target sequence [50]. KAPA2G with EvaGreen is highly sensitive as an intercalating dye-based system, and the fast-start polymerase allows for ultra-fast cycling protocols. Cai et al. (2019) [15] showed that EvaGreen-based systems can deliver quick, sensitive, and reliable results in microfluidic qPCR setups. Our screening supports their findings: AmpliTaq recipes like 3, 4, and 13 (Table A3, Supplementary Materials) displayed strong fluorescence signal and good amplification curves, both on-chip and on benchtop. Meanwhile, KAPA2G also produced accurate results, where recipes 4, 7, and 13 (Table A4, Supplementary Materials) showed high fluorescence increases and high-quality curve fits, especially on-chip. Both systems showcased good assay compatibility, where AmpliTaq offers consistency and specificity, while KAPA2G with EvaGreen excels in speed and sensitivity.

In food safety testing, both time and sensitivity are critical. Therefore, on-chip qPCR amplification using the intercalating dye-based system KAPA2G with EvaGreen was optimized and validated following preliminary and screening experiments. The assay optimization was needed as most of the qPCR master mix commercial kits were optimized for benchtop instruments that uses reaction volumes up to 10 μL larger than the ones on chip.

During optimization, the central composite rotatable design (CCRD) enabled a systematic exploration of reaction conditions for on-chip qPCR by modelling the effect of primer and polymerase concentrations on selected outcome measures. The resulting response surface plots pointed to a consistent trend: the most favourable amplification efficiencies were observed at lower primer concentrations and relatively high polymerase levels. Only PCR efficiency could be used as an outcome measure, since no significant difference between recipes could be found in C_t values. Likely, the concentration ranges tested were already nearly optimized, yielding low differences.

Given this information, three formulations were selected ("high-cost", "low-cost" and "unreliable") from the CCRD output for validation. While all three recipes produced amplification across the dilution series, only the "high-cost" and "low-cost" recipes showed consistent, specific signals across replicates and conditions.

The "unreliable" recipe initially appeared promising due to early C_t values and efficiency estimates close to 100 %. However, amplification was also observed in no-template controls (NTC) on benchtop. Gel electrophoresis (data non shown) confirmed that these products differed in size from the 82 bp target, indicating non-specific amplification, most likely from primer-dimer formation. These findings emphasize a key limitation of model-driven optimization: statistical predictions must always be validated experimentally, particularly in qPCR where non-specific reactions can mislead efficiency calculations. Several recent studies have highlighted the impact of primer concentration on dimer formation and false-positive signals in highly sensitive assays [51,52].

Ultimately, while CCRD modelling streamlined the development process and narrowed down the testing matrix, the incorporation of gel electrophoresis and NTC controls was critical in identifying the false efficiency from the "unreliable" formulation. These results underscore the importance of balancing sensitivity, speed, and specificity, particularly for qPCR-based food safety assays where both accuracy and turnaround time are essential.

Following optimization, experiments showcased sensitivity of the assay down to four genome equivalents (GE) per chip (1.8 μL volume) with a 95 % certainty rate. During these experiments, the dilution series – with minimum three replicates per concentration – revealed an efficiency of 95.9 %. Additionally, a high specificity of 95 % was attained by testing the amplification system on 20 target and 20 non-target DNAs in concentrations of 100 and 1000 GE per chip, respectively [34].

The main advantages of performing on-chip qPCR (when compared to the conventional protocol using a 96-well plate) are the lower reagents, volume and reaction completion time. Combined, these advantages also decrease total cost of the assay. When compared to other conventional methods of detection for foodborne pathogens like enzyme-linked immunosorbent assays (ELISA), next generation sequencing (NGS) and culture-based detection, the decrease in time and money of on-chip qPCR becomes even more apparent [4,6]. Table A11 (Supplementary material) compares the costs, advantages and disadvantages of conventional methods compared to the on-chip qPCR proposed in this paper [53,54].

One of the main challenges when performing on-chip PCR is the reagents handling, that is currently executed using a manual pipette as sample dispenser. However, to increase the throughput analysis the number handling steps needs to scale up, meaning that different solutions need to be considered to accurately manipulate samples from

different sources. One approach is to use a pipetting robot to manipulate distinct assays on different chip cartridges with minimal chance of pipetting errors. However, most automated dispensing systems are bulky and costly. But there have been efforts to miniaturize it, making this approach more affordable and portable [55]. The use of a dispensing robot allows the loading of different chips in parallel.

Another aspect to consider is the ability to perform temperature cycling and fluorescence monitoring on several chips in parallel. At this moment our commercial partner (MiDx, Leuven Belgium) does not offer this possibility but with an increasing demand it can be offered as an upgraded version to the current instrument in use.

The assay reproducibility was achieved when performing an appropriate on-chip surface cleaning to remove potential polymer residues from the fabrication step (as the O_2 plasma cleaning step described on section "2.1.3.1 Microfluidic chip available at the materials and methods" section). The results presented here showed a good reproducibility on the amplification curves (see Section 3.3 on the results section). The addition of the right additives to the master mix solution (as bovine serum albumin on the right concentration) passivates the chip surface against unwanted adsorption.

The fabrication flow employed by our chip supplier (MiDx, Leuven Belgium) is based on photolithography to transfer the channels, inlet ports and silicon-glass anodic bonding to seal the fabricated structures (as described in the literature [56,57]). During this study more than 300 chips were used (to validate the tool and assay) with a minimal failure rate (lees then 20 units had issues mainly due to the chip cartridge assembly failure). As the demand for on chips diagnostics increases the cost per unit will decrease [58].

All data presented in this paper were acquired using chips made in silicon due to its optimal thermal properties allowing fast thermal cycling and good reaction efficiency reproducibility. The cost per chip provided by the partner was accessible (€ 50/chip) due to the small footprint of the silicon layer. Furthermore, as production scales up from laboratory prototyping to industrial manufacturing, the high-volume production would enable process optimization, automated assembly, and bulk material procurement, all contributing to greater affordability and market accessibility [58]. While this procedure improved reproducibility of experiments, it also increased the demand of time and effort. The plastic foil interposer on-chip (with embedded channels) facilitated the reagents loading by the need of a single drop at the foil inlet port.

The loading efficiency of the chips was 95 % by the end of the assay optimization, making the reagent loading achievable to a final user without intensive training. The tool in use to perform the temperature cycling and fluorescence reading was compact and allowed a faster reaction completion (40 min faster than the benchtop tool). By using dedicated image and statistics software packages (Image J and R code) the amplification efficiency from each on chip qPCR was determined in a semi-automated way with minimal interaction from the final user.

Despite the current limitations of the system imposed by small-scale production and limited diversity in sample testing, we believe the on-chip qPCR method discussed here holds promise in detecting bacterial pathogens in a multitude of matrices. Upscaling of the production process will reduce the overall costs increasing accessibility making sensitive and fast pathogens detection by on chip qPCR accessible in more diverse locations.

5. Conclusions

An assay validation routine for detection of *egc*- positive *S. aureus* by qPCR using silicon chips as reaction chambers for the amplification step was proposed. The optimization led to amplification results with good sensitivity (down to 2.22 genome equivalents/μL detection) and reproducibility under reduced volume (1.8 μL) and completion time (19 min) when compared to the golden standard benchtop tool approach. This method can be used for the optimization of other assays targeting different templates (like bacterial strains) moving towards transferring the benchtop tool qPCR recipes into chip devices making the overall protocol more accessible for food pathogens detection regarding costs and overall timing.

Declaration of generative AI and AI-assisted technologies in the manuscript preparation process

During the preparation of this work the authors used [M365 Copilot] to modify an image (add colours and 3-d effects to an image) (graphical abstract). After using this tool/service, the authors reviewed and edited the content as needed and take full responsibility for the content of the published article.

Funding

This research was funded by Horizon 2020 Europe frame agreement, grant number 101059813.

CRediT authorship contribution statement

Ana João Pereira: Writing – original draft, Visualization, Supervision, Project administration, Methodology, Formal analysis, Data curation, Conceptualization. **Steven Schoonderwoerd:** Writing – original draft, Visualization, Methodology, Investigation, Formal analysis. **Rodrigo Sergio Wiederkehr:** Writing – review & editing, Writing – original draft, Formal analysis, Data curation, Conceptualization. **Daniele Chieffi:** Writing – review & editing, Writing – original draft, Methodology. **Vincenzina Fusco:** Writing – review & editing, Writing – original draft, Methodology, Funding acquisition. **Gabriela Vollet Marson:** Writing – review & editing, Visualization, Supervision, Resources, Project administration, Methodology, Formal analysis, Data curation, Conceptualization.

Declaration of competing interest

The authors have no competing interests to declare that are relevant to the content of this article.

Acknowledgements

We would like to thank Marcel Tempelaars (Laboratory of Food Microbiology, Wageningen University & Research) for his scientific input and assistance in performing agarose gel electrophoresis to rule out primer-dimer issues encountered on benchtop qPCR during recipe selection for optimization.

Supplementary materials

Supplementary material associated with this article can be found, in the online version, at doi:10.1016/j.talo.2026.100633.

Data availability

The data that has been used is confidential.

References

[1] M. Aladhadh, A review of modern methods for the detection of foodborne pathogens, Microorganisms 11 (2023), https://doi.org/10.3390/microorganisms11051111.
[2] N.C. Cady, V. Fusco, G. Maruccio, E. Primiceri, C.A. Batt, Micro- and nanotechnology-based approaches to detect pathogenic agents in food, Nanobiosensors (2017) 475–510, https://doi.org/10.1016/B978-0-12-804301-1.00012-6.
[3] M.J. Chapela, A. Garrido-Maestu, A.G. Cabado, Detection of foodborne pathogens by qPCR: a practical approach for food industry applications, Cogent. Food Agric. 1 (2015), https://doi.org/10.1080/23311932.2015.1013771.

[4] S. Hameed, L. Xie, Y. Ying, Conventional and emerging detection techniques for pathogenic bacteria in food science: a review, Trend. Food Sci. Technol. 81 (2018) 61–73, https://doi.org/10.1016/J.TIFS.2018.05.020.

[5] A. Jahangiri, S. Dahaghin, E. Malekara, R. Halabian, M. Mahboobi, E. Behzadi, H. Sedighian, Highly sensitive detection of *Staphylococcus aureus* α-hemolysin protein (Hla or α-toxin) by apta-qPCR, J. Microbiol. Method. 229 (2025) 107084, https://doi.org/10.1016/J.MIMET.2024.107084.

[6] J.W.F. Law, N.S.A. Mutalib, K.G. Chan, L.H. Lee, Rapid methods for the detection of foodborne bacterial pathogens: principles, applications, advantages and limitations, Front. Microbiol. 5 (2014), https://doi.org/10.3389/fmicb.2014.00770.

[7] Y. Zhao, Y. Shang, Z. Wang, Z. Wang, J. Xie, H. Zhai, Z. Huang, Y. Wang, Q. Wu, Y. Ding, J. Wang, The recent advances of high-throughput biosensors for rapid detection of foodborne pathogens, TrAC- Trends Anal. Chem. 176 (2024), https://doi.org/10.1016/j.trac.2024.117736.

[8] D. Gao, Z. Ma, Y. Jiang, Recent advances in microfluidic devices for foodborne pathogens detection, TrAC - Trends Anal. Chem. 157 (2022), https://doi.org/10.1016/j.trac.2022.116788.

[9] J.W.F. Law, N.S.A. Mutalib, K.G. Chan, L.H. Lee, Rapid methods for the detection of foodborne bacterial pathogens: principles, applications, advantages and limitations, Front. Microbiol. 5 (2014), https://doi.org/10.3389/fmicb.2014.00770.

[10] X. Zhao, C.W. Lin, J. Wang, D.H. Oh, Advances in rapid detection methods for foodborne pathogens, J. Microbiol. Biotechnol. 24 (2014) 297–312, https://doi.org/10.4014/jmb.1310.10013.

[11] V. Fusco, G.M. Quero, Culture-dependent and culture-independent nucleic-acid-based methods used in the microbial safety assessment of milk and dairy products, Compr. Rev. Food Sci. Food Saf. 13 (2014) 493–537, https://doi.org/10.1111/1541-4337.12074.

[12] H. Gudnason, M. Dufva, D.D. Bang, A. Wolff, Comparison of multiple DNA dyes for real-time PCR: Effects of dye concentration and sequence composition on DNA amplification and melting temperature, Nucleic Acids Res. 35 (2007), https://doi.org/10.1093/nar/gkm671.

[13] J. Liu, C. Hansen, S.R. Quake, Solving the "world-to-chip" interface problem with a microfluidic matrix, Anal. Chem. 75 (2003) 4718–4723, https://doi.org/10.1021/ac0346407.

[14] A. Sposito, V. Hoang, D.L. DeVoe, Rapid real-time PCR and high resolution melt analysis in a self-filling thermoplastic chip, Lab Chip 16 (2016) 3524–3531, https://doi.org/10.1039/C6LC00711B.

[15] Q. Cai, M. Fauvart, R.S. Wiederkehr, B. Jones, P. Cools, P. Goos, M. Vaneechoutte, T. Stakenborg, Ultra-fast, sensitive and quantitative on-chip detection of group B streptococci in clinical samples, Talanta 192 (2019) 220–225, https://doi.org/10.1016/J.TALANTA.2018.09.041.

[16] Y. Su, X. Jin, F. Yang, X. Liu, F. Li, Q. Zhao, J. Hou, S. Zhang, H. Li, G. Huang, R. Fu, A compact microfluidic platform for rapid multiplex detection of respiratory viruses via centrifugal polar-absorbance spectroscopy, Talanta 280 (2024), https://doi.org/10.1016/j.talanta.2024.126733.

[17] R. Fu, Q. Li, R. Wang, N. Xue, X. Lin, Y. Su, K. Jiang, X. Jin, R. Lin, W. Gan, Y. Lu, G. Huang, An interferometric imaging biosensor using weighted spectrum analysis to confirm DNA monolayer films with attogram sensitivity, Talanta 181 (2018) 224–231, https://doi.org/10.1016/j.talanta.2017.12.066.

[18] N. Li, Y. Zhang, H. Wang, X. Xu, X. Huo, J. Wang, Y. Xu, A chip-based universal strategy to realize multiplex PCR by using wax films for sealing and controllable release of primers, Biosens. Bioelectron. 269 (2025), https://doi.org/10.1016/j.bios.2024.116921.

[19] V. Fusco, G. Blaiotta, K. Becker, Staphylococcal food poisoning. Food Safety and Preservation, 2018, pp. 353–390. 10.1016/B978-0-12-814956-0.00012-3.

[20] A.A. Al-Nabulsi, T.M. Osaili, R.A. AbuNaser, A.N. Olaimat, M. Ayyash, M.A. Al-Holy, K.M. Kadora, R.A. Holley, Factors affecting the viability of Staphylococcus aureus and production of enterotoxin during processing and storage of white-brined cheese, J. Dairy Sci. 103 (2020) 6869–6881, https://doi.org/10.3168/jds.2020-18158.

[21] D. Chieffi, F. Fanelli, G.S. Cho, J. Schubert, G. Blaiotta, C.M.A.P. Franz, J. Bania, V. Fusco, Novel insights into the enterotoxigenic potential and genomic background of Staphylococcus aureus isolated from raw milk, Food Microbiol. 90 (2020) 103482, https://doi.org/10.1016/J.FM.2020.103482.

[22] K. Umeda, H.K. Ono, T. Wada, D. Motooka, S. Nakamura, H. Nakamura, D.L. Hu, High production of egc2-related staphylococcal enterotoxins caused a food poisoning outbreak, Int. J. Food Microbiol. 357 (2021) 109366, https://doi.org/10.1016/J.IJFOODMICRO.2021.109366.

[23] K. Umeda, H. Nakamura, K. Yamamoto, N. Nishina, K. Yasufuku, Y. Hirai, T. Hirayama, K. Goto, A. Hase, J. Ogasawara, Molecular and epidemiological characterization of staphylococcal foodborne outbreak of Staphylococcus aureus harboring seg, sei, sem, sen, seo, and selu genes without production of classical enterotoxins, Int. J. Food Microbiol. 256 (2017) 30–35, https://doi.org/10.1016/J.IJFOODMICRO.2017.05.023.

[24] G. Zhao, Z. Lou, Z. Zhu, X. Lai, J. Li, X. Lou, L. Huang, Q. Chen, Epidemiological and molecular evidence of foodborne poisoning outbreak caused by enterotoxin gene cluster-harboring Staphylococcus aureus of new sequence type 7591, Int. J. Infect. Dis. 135 (2023) 132–135, https://doi.org/10.1016/J.IJID.2023.08.005.

[25] S. Jarraud, M.A. Peyrat, A. Lim, A. Tristan, M. Bes, C. Mougel, J. Etienne, F. Vandenesch, M. Bonneville, G. Lina, A highly prevalent operon of enterotoxin gene, forms a putative nursery of superantigens in staphylococcus aureus, J. Immuno. 166 (2001) 669–677, https://doi.org/10.4049/jimmunol.166.1.669.

[26] S.T.A. Dantas, L.B.B. Silva, L.T.S. Takume, B.F. Rossi, E.C.R. Bonsaglia, A. Fernandes Júnior, J.C.F. Pantoja, M.V. dos Santos, J.L. Gonçalves, A.O.B. Ribon, N.C.C. Silva, V.L.M. Rall, Diversity of Staphylococcus aureus enterotoxin genes and its potential impact on severity of mastitis in dairy cows, Microb. Pathog. 198 (2025) 107119, https://doi.org/10.1016/J.MICPATH.2024.107119.

[27] A.J. Fischer, S.H. Kilgore, S.B. Singh, P.D. Allen, A.R. Hansen, D.H. Limoli, P. M. Schlievert, High prevalence of Staphylococcus aureus enterotoxin gene cluster superantigens in cystic fibrosis clinical isolates, Genes (Basel) 10 (2019), https://doi.org/10.3390/genes10121036.

[28] L. Blicharz, M. Żochowski, K. Szymanek-Majchrzak, J. Czuwara, M. Goldust, K. Skowroński, G. Młynarczyk, M. Olszewska, Z. Samochocki, L. Rudnicka, Enterotoxin gene cluster and selX are associated with atopic dermatitis severity—A cross-sectional molecular study of Staphylococcus aureus superantigens, Cells 11 (2022), https://doi.org/10.3390/cells11233921.

[29] V. Fusco, G.M. Quero, M. Morea, G. Blaiotta, A. Visconti, Rapid and reliable identification of Staphylococcus aureus harbouring the enterotoxin gene cluster (egc) and quantitative detection in raw milk by real time PCR, Int. J. Food Microbiol. 144 (2011) 528–537, https://doi.org/10.1016/J.IJFOODMICRO.2010.11.016.

[30] D. Chieffi, D. Bongiorno, A. Licitra, F. Campanile, V. Fusco, A novel approach based on real-time PCR with high-resolution melting analysis for the simultaneous identification of Staphylococcus aureus and Staphylococcus argenteus, Foods 13 (2024), https://doi.org/10.3390/foods13183004.

[31] T.B. Christensen, C.M. Pedersen, K.G. Gröndahl, T.G. Jensen, A. Sekulovic, D. D. Bang, A. Wolff, PCR biocompatibility of lab-on-a-chip and MEMS materials, J. Micromech. Microeng. 17 (2007) 1527–1532, https://doi.org/10.1088/0960-1317/17/8/015.

[32] I. Erill, S. Campoy, N. Erill, J. Barbé, J. Aguiló, Biochemical analysis and optimization of inhibition and adsorption phenomena in glass-silicon PCR-chips, Sens. Actuators B Chem. 96 (2003) 685–692, https://doi.org/10.1016/S0925-4005(03)00522-7.

[33] M.I. Rodrigues, A.F. Iemma. Experimental Design Process Optimization, 1st ed., CRC Press, Taylor & Francis Group, Boca Raton, 2014.

[34] S. Broeders, I. Huber, L. Grohmann, G. Berben, I. Taverniers, M. Mazzara, N. Roosens, D. Morisset, Guidelines for validation of qualitative real-time PCR methods, Trends Food Sci. Technol. 37 (2014) 115–126, https://doi.org/10.1016/J.TIFS.2014.03.008.

[35] FAO, Codex alimentarius: guidelines on performance criteria and validation of methods for detection, identification and quantification of specific DNA sequences and specific proteins, Foods (2010).

[36] FAO, IFAD, UNICEF, WFP, WHO, The State of Food Security and Nutrition in the World 2024 - Financing to end hunger, food insecurity and malnutrition in all its form, FAO; IFAD; UNICEF; WFP; WHO;, 2024. https://doi.org/10.4060/cd1254en.

[37] S.P. Oliver, B.M. Jayarao, R.A. Almeida. Review Foodborne Pathogens in Milk and the Dairy Farm Environment: Food Safety and Public Health Implications, 2005.

[38] C. Wood, J. Sahl, S. Maltinsky, B. Coyne, B. Russakoff, D.P. Yagüe, J. Bowers, T. Pearson, SaQuant: a real-time PCR assay for quantitative assessment of Staphylococcus aureus, BMC Microbiol. 21 (2021), https://doi.org/10.1186/s12866-021-02247-6.

[39] P. Heng, J. Liu, Z. Song, C. Wu, X. Yu, Y. He, Rapid detection of Staphylococcus aureus using a novel multienzyme isothermal rapid amplification technique, Front. Microbiol. 13 (2022), https://doi.org/10.3389/fmicb.2022.1027785.

[40] M. Smistad, M.K. Vatne, L. Sølverød, K.R. Dean, Sensitivity and specificity of bacterial culture, qPCR, and somatic cell count for detection of goats with Staphylococcus aureus intramammary infection using Bayesian latent class models, Prev. Vet. Med. 209 (2022) 105793, https://doi.org/10.1016/J.PREVETMED.2022.105793.

[41] B. Zhou, Q. Ye, M. Chen, F. Li, X. Xiang, Y. Shang, C. Wang, J. Zhang, L. Xue, J. Wang, S. Wu, R. Pang, Y. Ding, Q. Wu, Novel species-specific targets for real-time PCR detection of four common pathogenic Staphylococcus spp, Food Control 131 (2022) 108478, https://doi.org/10.1016/J.FOODCONT.2021.108478.

[42] S. Wei, C. Wang, P. Zhu, G. Zhou, W. Fu, X. Wu, A high-throughput multiplex tandem PCR assay for the screening of genetically modified maize, LWT 87 (2018) 169–176, https://doi.org/10.1016/J.LWT.2017.08.061.

[43] V. Garzarelli, M.S. Chiriacò, M. Cereda, G. Gigli, F. Ferrara, Ultrasensitive qPCR platform for rapid detection of bacterial contamination of raw biological samples at the point of care, Heliyon 9 (2023) e16229, https://doi.org/10.1016/J.HELIYON.2023.E16229.

[44] Z. Wang, W. Lu, X. Li, N. Xu, L. Lin, Q. Song, Y. Liu, Z. Hu, S. Guo, Y. Gao, W. Wen, Rapid detection of Salmonella and Staphylococcus aureus using a hand-held nucleic acid detection system, J. Food Saf. 44 (2024), https://doi.org/10.1111/jfs.13157.

[45] J. Treffon, N. Isserstedt-John, R. Klemm, C. Gärtner, A. Mellmann, Evaluation of a microfluidic-based point-of-care prototype with customized chip for detection of bacterial clusters, Microbiol. Spectr. 12 (2024), https://doi.org/10.1128/spectrum.00862-24.

[46] L. Cocolin, K. Rantsiou, Quantitative polymerase chain reaction in Food Microbiology, in: M. Filion (Ed.), Quantitative Real-Time PCR in Applied Microbiology, vii, Caister Academic Press, Norfolk, UK, 2012, pp. 122–149.

[47] J.A. Hennekinne, M.L. De Buyser, S. Dragacci, Staphylococcus aureus and its food poisoning toxins: Characterization and outbreak investigation, FEMS Microbiol. Rev. 36 (2012) 815–836, https://doi.org/10.1111/j.1574-6976.2011.00311.x.

[48] D. Rodríguez-Lázaro, E.A. Oniciuc, P.G. García, D. Gallego, I. Fernández-Natal, M. Dominguez-Gil, J.M. Eiros-Bouza, M. Wagner, A.I. Nicolau, M. Hernández, Detection and characterization of Staphylococcus aureus and methicillin-resistant S. aureus in foods confiscated in EU borders, Front. Microbiol. 8 (2017), https://doi.org/10.3389/fmicb.2017.01344.

[49] A.C.G. Foddai, I.R. Grant, Methods for detection of viable foodborne pathogens: current state-of-art and future prospects, Appl. Microbiol. Biotechnol. 104 (2020) 4281–4288, https://doi.org/10.1007/s00253-020-10542-x.
[50] M. Arya, I.S. Shergill, M. Williamson, L. Gommersall, N. Arya, H.R. Patel, Basic principles of real-time quantitative PCR, Expert Rev. Mol. Diagn. 5 (2005) 209–219, https://doi.org/10.1586/14737159.5.2.209.
[51] R.R. Garafutdinov, A.A. Galimova, A.R. Sakhabutdinova, The influence of quality of primers on the formation of primer dimers in PCR, Nucleosides Nucleotides Nucleic Acids 39 (2020) 1251–1269, https://doi.org/10.1080/15257770.2020.1803354.
[52] L.H. Jaeger, T.C. Nascimento, F.D. Rocha, F.M.P. Vilela, A.P. do N. Duque, L.M. Silva, L.R. Riani, J.P. Moreira, J.M. de A. Chagas, T.V. Pereira, C.G.P. Perches, A.S. A. Watanabe, L.F. Viccini, M.S. Silvério, J.O. do A. Corrêa, O. dos S. Pereira-Junior, F. Pittella, Adjusting RT-qPCR conditions to avoid unspecific amplification in SARS-CoV-2 diagnosis, Inter. J. Infect. Diseases 102 (2021) 437–439. 10.1016/J.IJID.2020.10.079.
[53] M.A. Haddad, H. Tarawneh, S. Abu-Romman, N. Akhter, J.A. Rather, Emerging analytical techniques for determination of foodborne pathogens and toxins: a review, Discover Food 5 (2025), https://doi.org/10.1007/s44187-025-00590-5.
[54] S.K. Urwyler, J. Glaubitz, Advantage of MALDI-TOF-MS over biochemical-based phenotyping for microbial identification illustrated on industrial applications, Lett. Appl. Microbiol. 62 (2016) 130–137, https://doi.org/10.1111/lam.12526.
[55] P. Dettinger, T. Kull, G. Arekatla, N. Ahmed, Y. Zhang, F. Schneiter, A. Wehling, D. Schirmacher, S. Kawamura, D. Loeffler, T. Schroeder, Open-source personal pipetting robots with live-cell incubation and microscopy compatibility, Nat. Commun. 13 (2022), https://doi.org/10.1038/s41467-022-30643-7.
[56] C. Iliescu, H. Taylor, M. Avram, J. Miao, S. Franssila, A practical guide for the fabrication of microfluidic devices using glass and silicon, Biomicrofluidics 6 (2012), https://doi.org/10.1063/1.3689939.
[57] X. Liu, A. Sun, J. Brodský, I. Gablech, T. Lednický, P. Vopařilová, O. Zítka, W. Zeng, P. Neužil, Microfluidics chips fabrication techniques comparison, Sci. Rep. 14 (2024), https://doi.org/10.1038/s41598-024-80332-2.
[58] H. Cong, N. Zhang, Perspectives in translating microfluidic devices from laboratory prototyping into scale-up production, Biomicrofluidics 16 (2022), https://doi.org/10.1063/5.0079045.